VOL. 14, NO. 1, JANUARY 2019 ISSN 1819-6608
ARPN Journal of Engineering and Applied Sciences

www.arpnjournals.com

STUDY THE CORROSION BEHAVIOR AND MICROSTRUCTURE OF Ti-5Al-2.5Fe-xMo ALLOYS FOR BIOMEDICAL APPLICATIONS

Nabeel Mohammed Abd Alkadim and Jassim Mohammed Salman
College of Materials Engineering, University of Babylon, Babylon, Iraq
E-Mail: nabeelmohammed666@gmail.com

ABSTRACT

This work is studied the effect of adding different percentages of molybdenum by powder metallurgy technique of Ti-5Al-2.5Fe-xMo alloys (x= 1,2 and 3wt%) on corrosion behavior and microstructure in different fluid body (artificial saliva and Hank's solutions).After specimens preparation, an examinations were done by using x-ray diffraction (XRD), scanning electron microscope(SEM), and light optical microscope(LOM). The corrosion properties of theTi-5Al-2.5Fe alloy and the Ti-5Al-2.5Fe alloys with Mo additives were examined by using electrochemical technique sat 37ºC, such as the potentiodynamic method and open circuit potential (OCP).The XRD and microstructure results show that comprises dominant α and minimal β phases at room temperature and the addition of Mo in these percentages does not have effect on the present phases. From the corrosion results can see in 3wt% Mo the alloys have less corrosion rate than the master or other percentage (1 wt% and 2 wt%) in all solutions (artificial saliva and Hank's solutions).

Keywords: corrosion behavior, powder metallurgy, Ti-5Al-2.5Fe alloy, molybdenum.

1. INTRODUCTION

Titanium and its alloys are currently the greatest attractive metallic biomaterials in contrast to the polymeric and ceramic biomaterials which have poor mechanical properties [1]. The greater physical phenomena of Ti alloys are that it is lightweight, has robust mechanical properties and, in particular, it has low density and low elastic modulus, which gives It a little thermal conductive coefficient (17 $w \cdot m^{-1} \cdot k^{-1}$) as compared with traditional metals. The chemical properties of Ti and its alloys include good corrosion resistance, good antibacterial properties, and high biocompatibility with humans. These features make titanium the preferred choice of implants in the human body [2].Titanium is currently used in cardiac catheters, however, it is corroded by body fluids, Containing proteins and chloride ions. Where, the metal is oxidized to the ions of that metal and the ratio of dissolved oxygen to hydroxide ions is reduced and this is done in the process of corrosion. Titanium decay products can cause Inflammation of the human body[3].Cellular and molecular interactions between implants and bone can be controlled to a certain extent through the properties of the surface of the cultivated materials. There are a range of properties of surface including physiochemical and biochemical which are responsible for biological execution such as protein uptake, cell correlation, and subsequent Osseo integration of titanium implants [4]. Ti-6Al-4V is the chief of biomedical titanium alloy for a long time. However, because of the toxicity issues that associated to the vanadium compounds, new types Of titanium alloys like Ti-5Al-2.5Fe and Ti-6Al-7Nb have been advanced. Both alloys offers good biocompatility and similar mechanical properties compared to Ti-6Al-4V[5].

In the present study, powder metallurgy (PM) was used for the manufacture of Ti-5Al-2.5Fe alloy from elemental Powders. Powder metallurgy provides close shape of the finished product with basic production parameters [6]. Also it provides using of 90% of raw material compared with casting. New materials can be developed and produced in a wide range of field in powder metallurgical techniques [7, 8]. The PM process principally consists of mixing powdered materials (blending), pressing to get the favorite shape (compaction), and heating and Soaking the compact to bond the powder (sintering). Optional post-processing operations i.e., machining, grinding, sizing, heat treatment etc, could be further employed. During sintering of the powdered compacts the important criteria for the proper distribution of the liquid phase throughout the solid matrix are: 1. melting of the liquid forming additives (elementalor master alloy) below normal sintering Temperatures, 2. good wettability of the molten phase, 3. removal of oxides, 4. the dissolution effects[9].

There are many papers focused on the development and improvement of Ti-5Al-2.5Fe alloy. Rodrigo et al.[10] dissolution of intermetallic powders of the Ti-5Al-2.5Fe alloy was studied during the process of sintering using the blended elemental technique (BE) where samples were sintered and cold pressed in the vacuumatmo sphere between 700 - 1400 oC and a 2 hours stay for each temperature, Ridvan *et al.* [11] studied the effect of sintering properties on Ti-5Al-2.5Fe alloy was prepared by powder metallurgy, where the powders were sintered by hot pressing with a vacuum atmosphere at the temperature of 950 ° C and stay of 3 hours, Do-Heon et al.[12] Verification of phase transformation (β to α) through the effect of oxygen content on Ti-5Al-2.5Fe alloy during continuous cooling by changing the oxygen content between (0.08 wt% – 0.41 wt%) and cooling rates of (0.05 ℃/s - 100 ℃/s), Ridvan *et al.* [13] investigate of cell toxicity response and the mechanical antibacterial properties of Ti-5Al2.5Fe alloy with different copper contents (1, 3 and 5 wt%)

In this research, all specimens were prepared by powder metallurgical technique and study the effect of

alloying elements additions (Molybdenum) on the biomedical Ti-5Al-2.5Fe alloy and the corrosion tests and microstructural properties are discussed.

2. EXPERIMENTAL WORK

A. Preparation of samples

The master alloy compose of titanium powder with purity of 99.9% and particle size 25µm, aluminum powder with purity of 99% and particle size5.6µm, iron powder with purity of 99.7% and particle size 45µm. The percentage of master alloy(which has the code B) is (92.5%Ti-5%Al-2.5%Fe), then an addition of alloying elements in different percentages to the master alloy in order to prepare other alloys specimens are accomplished as shown in Table-1.

Table-1. Alloying element in different percentages to the master samples.

Alloying element	Particle size, µm	Purity %	Percentage wt %	Result alloys wt%	Code alloy
Mo	18	99.9	1%	91.5Ti-5Al-2.5Fe-1Mo	M1
			2%	90.5Ti-5Al-2.5Fe-2Mo	M2
			3%	89.5Ti-5Al-2.5Fe-3Mo	M3

After selecting the weighted percentages for each specimen the material powder was weighted by using the sensitive balance, the total weight of each specimen is 4gm. In order to obtain a uniform distribution of the powders and to achieve good mixing between elements, the specimens powders are mixed in a ball mill for 4 h at high level of speed for each specimen, Finally a homogenous powder is obtained and its ready for pressing process.

Pressing process includes compaction of the powder of each specimens by using the Punch and die (made from tool steel) with die diameter of 13 mm, and by using the hydraulic press machine as well. The powders were pressed under pressure of 850 MPa for 5 min and then specimens with diameter of 13mm and 5mm in height was produced.

The sintering process has been carried out under vacuum conditions by using vacuum tube furnace. The sintering process include heating the specimens from room temperature to 500℃ and Soaking for (2) hours, after that, heating from temperature 500° C to 850° C and Soaking for (6) hours then slow cooling inside the furnace with continues vacuum circumstances to the room temperature.

B. Microstructure characterization

-Microstructure observation

The microstructure of the alloy specimen was observed and studied using(LOM) and (SEM) before and after sintering process(the M3 was chosen with the base alloy B for these tests) and corrosion test. The specimens were grinded with the help of (220, 320, 600, 800, 1000,1200,1500,2000 and 2500) grit silicon carbide papers. Then they were polished with a diamond past of 15 µm to get a bright mirror finish for the last step. Specimens were etched using the following solutions shown in Table-2 [14]. The prepared specimens were swabbed in the etching solution for 20 seconds, then washed with distilled water and dried, which make them ready for microstructure observations.

Table-2. Chemical composition of etching solution.

No.	Constituents	ml
1	Hf	2
2	HNO_3	6
3	Distilled water	92

-X-ray diffraction

X-ray diffraction analysis has been performed on specimen to determine the existing phases (the M3 was chosen with the base alloy B for these tests). X-ray diffraction device used is (Lab X, XRD - 6000) with 40 Kv and 30 mA .Scanning speed 5° per minute was used (0 ° - 120 °) was the range of the diffraction angle.

C. Corrosion test

The corrosive behavior of Ti-5Al-2.5Fe alloy studied in two different solutions includes (artificial saliva and Hank's solutions). The chemical composition of Hank's and artificial saliva solutions is illustrated in Tables (3) and (4) respectively [15]. The preparation of solution was done by adding the specific amount of each constituent for each solution to a liter of deionized water and stirred for about 30 minutes at room temperature on a magnetic stirrer.

Table (3) : Chemical composition of artificial saliva

NO.	Constituents	(g/l)
1	KCl	1.5
2	$NaHCO_3$	1.5
3	$NaH_2PO_4H_2O$	0.5
4	HSCN	0.5
5	Lactic acid	0.9

Table (4) : Chemical composition of Hank's solution

NO.	Constituents	(g/l)
1	NaCl	8
2	$CaCl_2$	0.14
3	KCl	0.4
4	$NaHCO_3$	0.35
5	Glucose	1
6	$MgCl_2.6H_2O$	0.1
7	$Na_2HPO_4.H_2O$	0.06
8	KH_2PO_4	0.06
9	$MgSO_4.7H_2O$	0.06

-Open circuit potential (OCP)

The tests were carried out with the specimens immersed inartificial saliva and Hank's solutions. A 500 ml capacity glass electrolytic cell is used. Where the working electrode voltage is measured according to a (Saturated Calomel electrode) (S.C.E.). The voltmeter is connected between the reference electrode and the working electrode. For each specimen(2-4)hours open circuit potential measurement was performed. The first record was taken immediately after the immersion then the voltage was monitored for the entire period of test at an interval of (5 min).

-Potentiodynamic polarization

Electrochemical experiments were performed which containing three-electrode cell and electrolytes similar to nature (artificial saliva and Hank's solutions). The Assistant electrode was the (pt), the (S.C.E.) was the reference electrode, and the working electrode (specimen) according to American Society for Testing and Materials (ASTM). Both of the corrosion potential ($E_{corr.}$) and the corrosion current density ($I_{corr.}$) were calculated through the polarization curves using the Julius Tafel curve (anodic and cathodic branches)

The test was started by using 0.4 mV /s as the scanning rate from 350 mV bottom the (ocp) and continued test up to 350 mV above the (ocp The following equation can calculate the rate of erosion [16].

Corrosion Rate (mpy) =0.13. (I_{corr}).(EW)/ ρ .....(1)

Where: (I_{corr}) is corrosion current density ($\mu A/cm^2$)

(mpy) is Corrosion rate (mils per year)

0.13 is metric and time conversion factor

EW is equivalent weight (g/eq.)

ρ is density (g/cm^3)

3. RESULTS AND DISCUSSIONS

A. Microstructure characterization

-Optical microscope and scanning electron microscope

Light optical microscope (LOM) and scanning electron microscope (SEM) have been used to get the microstructure of the etched specimens. The specimens have been etched to reveal the grain boundaries in the microstructure and pores of different size are irregular.

The microstructure revealed that all the specimens alloys haveconsist mainly of two phases (α + β) structure at room temperature as shown in Figure (1). Compared with the master specimen, the addition of Mo elements lead to increasing the dark reign (β- phase) due to the effect of Mo as the Beta stabilizer elements. This fact is similar to in alpha-beta and beta alloys, some equilibrium beta is present at room temperature[17].

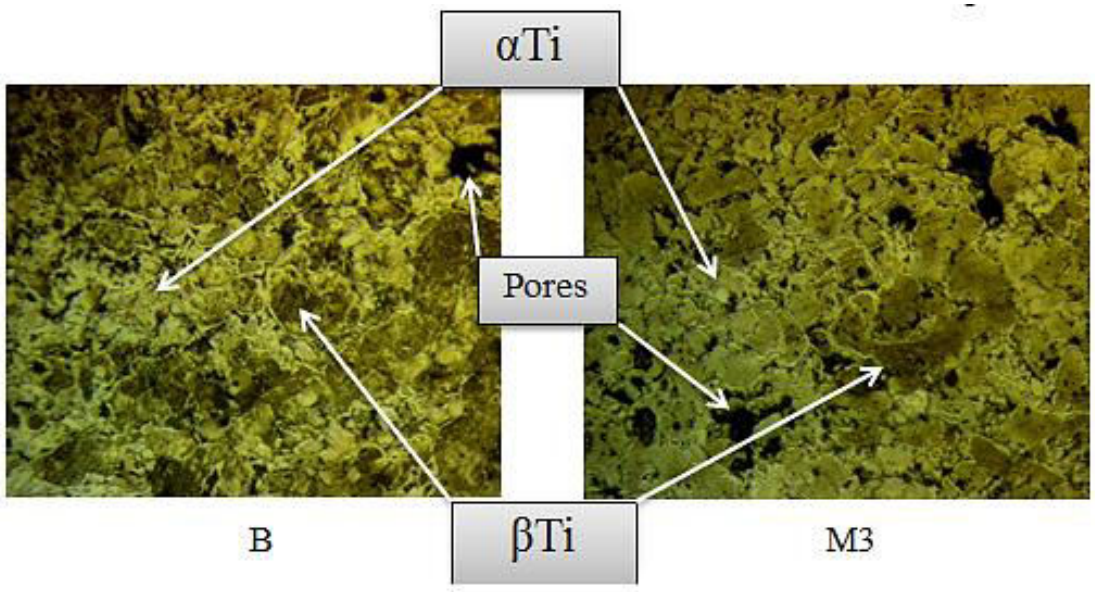

Figure-1. Microstructure for B and M3 alloys after sintering and etching (different magnification 100X-200X respectively).

SEM images are very sensible to the chemical composition as a result the microstructure of sintered specimens showed a multiphase structure in which the two phases (αTi and βTi), thus confirming the XRD results.

SEM images of etched alloys showed grain boundaries and pores in different sizes.

Figures (2) and (3) illustrates SEM images of etched alloys showed grain boundaries and pores in different sizes.

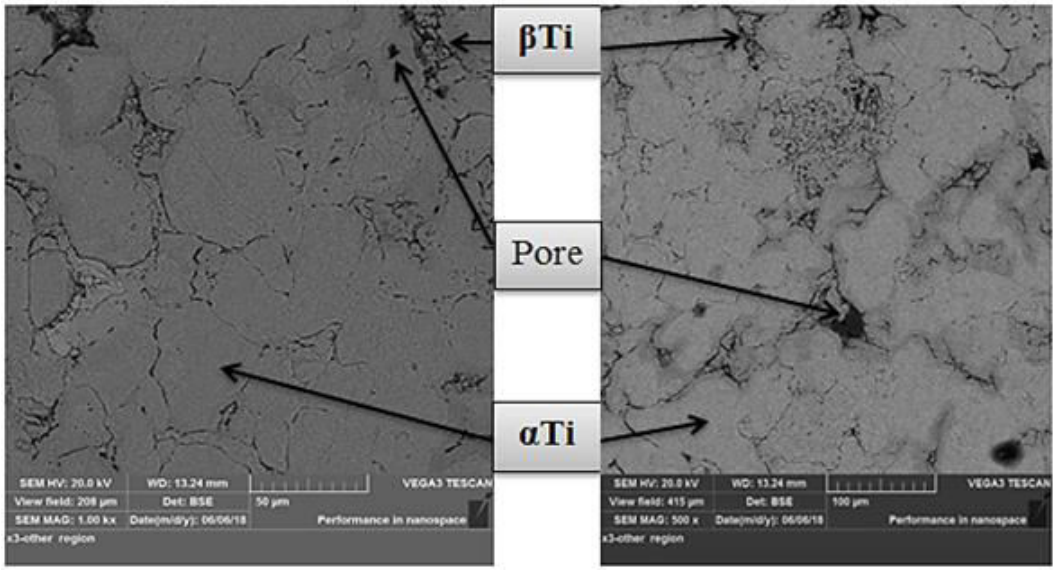

Figure-2. SEM images for etched B alloy.

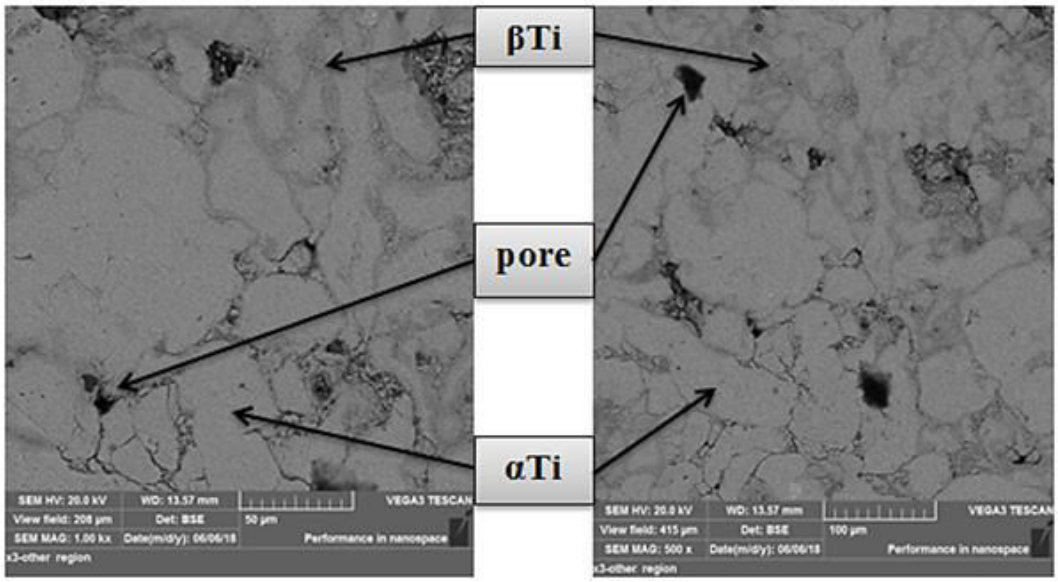

Figure-3. SEM images for etched M3 alloy.

- X-ray diffraction analysis

Phase transformation is diffusion process and needs a high temperature to occur. Figures (4) and (5) illustrated the XRD patterns for B and M3 alloys respectively after sintering at 850 C° for 6hours under vacuum conditions. It can be observed that all Ti, Al and Fe transformed to (αTi), (βTi), (Ti_3Al) and (Ti_2Al_5) phases.

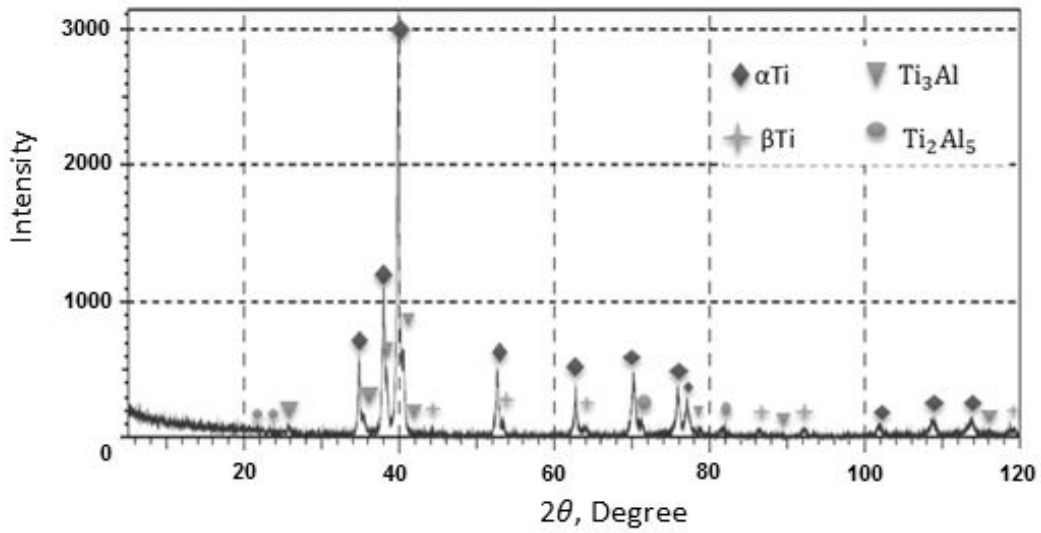

Figure-4. XRD pattern for B after sintering process.

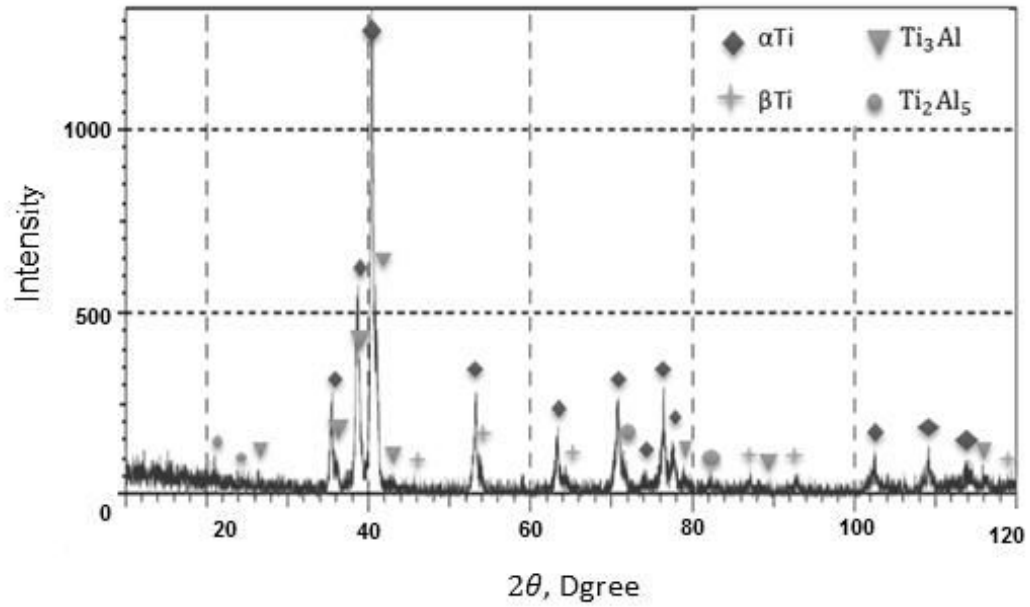

Figure-5. XRD pattern for M3 alloy after sintering.

B. CORROSION TEST

-Open circuit potential (OCP)-time measurement

The OCP-time is measured with respect to SCE in artificial saliva and Hank's solutions at 37 C°±2 for tested alloys. Figures (6) and (7) respectively displays the evolution of the potential corrosion of the alloys throughout the time in these solutions. The time period from (0 up to 290 min) and with interval of 5 min were potentially reported. The mean values of the OCP were recorded by using two samples for each alloy.

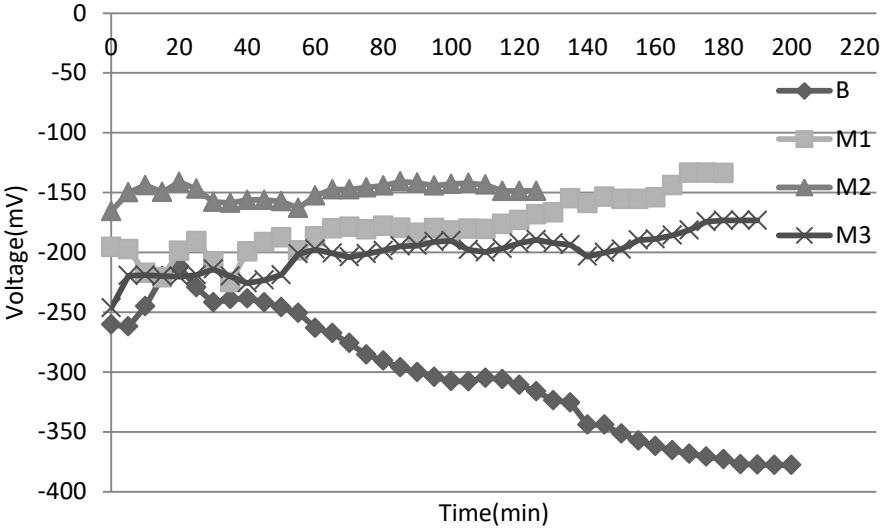

Figure-6. The OCP-time in hank's solution at 37±2 C°.

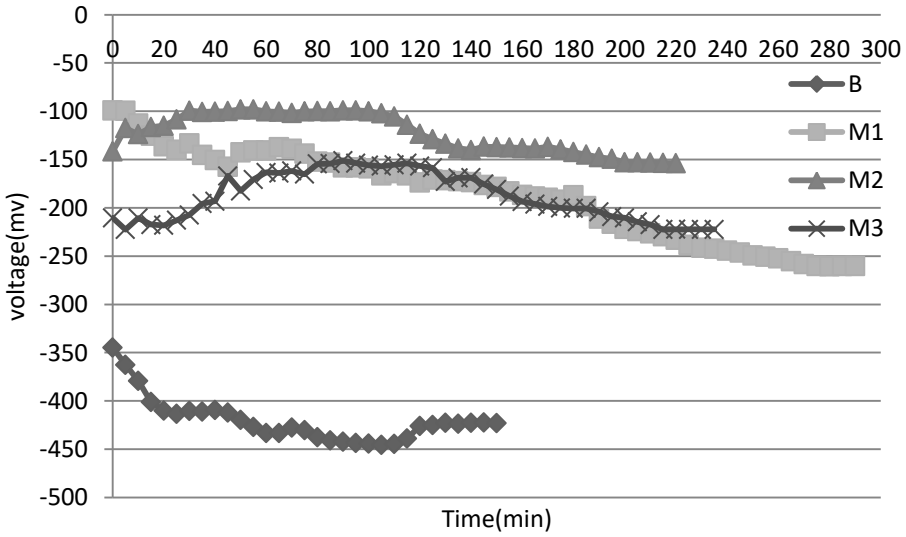

Figure-7. The OCP-time in artificial saliva at 37±2 C°.

In order to understand the stability of an alloy Ti-5Al-2.5Fe in the solutions of the human body, it is necessary to know its behavior in the environment of body fluids, This is done by the open-circuit potential as time which is considered one of the simple ways to study the formation of a protective layer and passivation of implants in Hank's and artificial saliva solutions. The above figures indicate to a rising of potential towards the positive direction where the surface of the implant is covered with a protective layer. Submerged alloys can be seen in the artificial saliva solution oriented to the negative direction and have a high negative value of (E_{ocp}) compared to the submerged alloys with Hank solution. The evolution of E_ocp of (B, M1, M2 and M3) alloys immersed in artificial saliva and Hank's solutions showed many deviations, Suggesting that the oxide layer formed on the surface of the implant is collapsed and formed, is that attributed to the processes of dissolution and rebuilding the protective layer. The presence of sulfur ions and chlorides in hostile solutions, in which the implants are immersed, is the cause of this behaviour [18].

-Potentiodynamic polarization

The corrosion behaviour of all the used alloys in Hank's and artificial saliva solutions has been studied.

The corrosion parameters are corrosion current density (I_{corr}), corrosion potential (E_{corr}), and (corrosion rate) resulted from the corrosion test for the specimens in the mentioned solutions at 37C° were illustrated in Tables (5) and (6).

From Table-5 it can be seen that there is a significant improvement in corrosion resistance of the alloys with different additives of Mo (M1-28.21%, M2-

89.33% & M3-150.22%) and I_{corr} for specimens are graded from 14.42 (μA/cm²) for M1 alloy to 7.05 (μA/cm²) for M3 alloy which are lower than $I_{corr}$for B alloy which is 19.28 (μA/cm²). However the E_{corr} values for M alloys is graded from -270.5mV for M1 to -203.7mv for M3 which are higher than E_{corr} for B alloy which is -187.0mV.

Table-5. Shows the corrosion current density (I_{corr}) corrosion potential (E_{corr}) and corrosion rate for all used alloys in Hank's solution at 37 C°.

Alloy	Sample code	I_{corr} (μA/cm²)	E_{corr} (mV)	Corrosion rate (mpy)	Improvement percentage%
ISO 5832-10	**B**	**19.28**	**-187.0**	**0.0568**	
M	**M1**	**14.42**	**-270.5**	**0.0443**	**28.21**
	M2	**9.68**	**-207.4**	**0.0300**	**89.33**
	M3	**7.05**	**-203.7**	**0.0227**	**150.22**

From Table-6 it can be noted that the improvement of corrosion resistance for Ti-5Al-2.5Fe alloy is lower than Ti-5Al-2.5 Fe alloys with Mo additives in artificial saliva (M1-13.43%, M2-63.81% & M3-90.80%). I_{corr} for Mo specimens are graded from 14.29(μA/cm²) for M1 alloy to 8.12 (μA/cm²) for M3 alloy which are more lower than I_{corr} for B alloy which is around 16.92 (μA/cm²). However the E_{corr}values for M alloys are graded from -323.7mV for M1 to -195.5mv for M3 which are significantly lower than $E_{corr}$for B alloy which is around -430.2mV.

Table-6. Shows the corrosion current density (I_{corr}), corrosion potential (E_{corr}) and corrosion rate for all alloys used in this work in artificial saliva at 37C°.

Alloy	Sample code	I_{corr} (μA/cm²)	E_{corr} (mV)	Corrosion rate (mpy)	Improvement percentage, %
ISO 5832-10	B	16.92	-430.2	0.0498	
M	M1	14.29	-323.7	0.0439	13.43
	M2	9.79	-306.8	0.0304	63.81
	M3	8.12	-195.5	0.0261	90.80

In previous research, the corrosion rate was found to be strongly related to pH, where corrosion rate decreased with the increase of pH, i.e., an inverse relationship. In our study, the pH of artificial saliva and Hank's solutions at 37C°±2 were 6.7 and 7.4 respectively [19]. From the two tables above it can be seen that there is a slight decrease in corrosion current and corrosion rate for B,M1,M2 and M3 specimens in Hank's solution as compared to specimens in artificial saliva solution.

Tables (5), (6) shows improvement in corrosion resistance of Ti-5Al-2.5Fe alloys with different additives of Mo in two corroded solutions as compared with Ti-5Al-2.5Fe alloy. Also the corrosion rate decreases as the Mo content increases as shown in Figure-8.

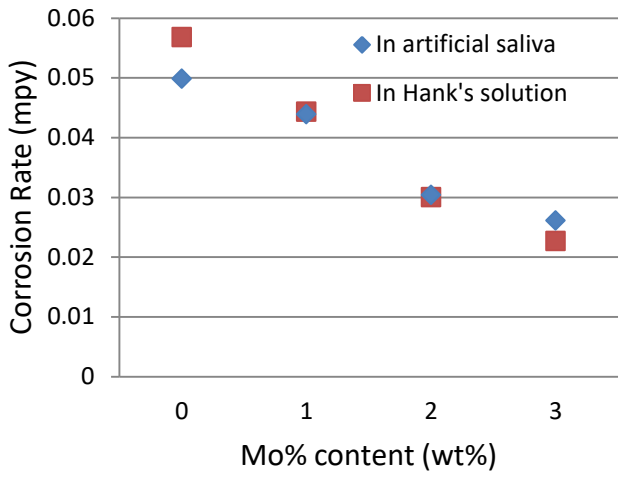

Figure-8. The effect of Mo content on corrosion rate of B, M1, M2 and M3 alloys in artificial saliva and Hank's solutions at 37 C°±2.

It's noticed in Figures (9) and (10) which represent polarization curves for alloys in two solutions (artificial saliva and Hank's solutions). Shows the potentiodynamic polarization curves of Ti-5Al-2.5Fe-xMo(X= 1, 2 and 3) alloys with different solutions at 37 C°±2. The nature of polarization curves is various between Ti-5Al-2.5Fe alloy andTi-5Al-2.5Fe-xMo alloys. In the Tafel curve, the base specimen is transferred directly to the passive region. However, in order for the Ti-5Al-2.5Fe-xMo specimens to tend to passivation, it must undergo several active-passive transitions. Therefore, until the low current density is obtained, the protective layer on the submerged specimen must be sufficiently integrated. Therefore, as the addition of molybdenum increases, the protective layer increases.

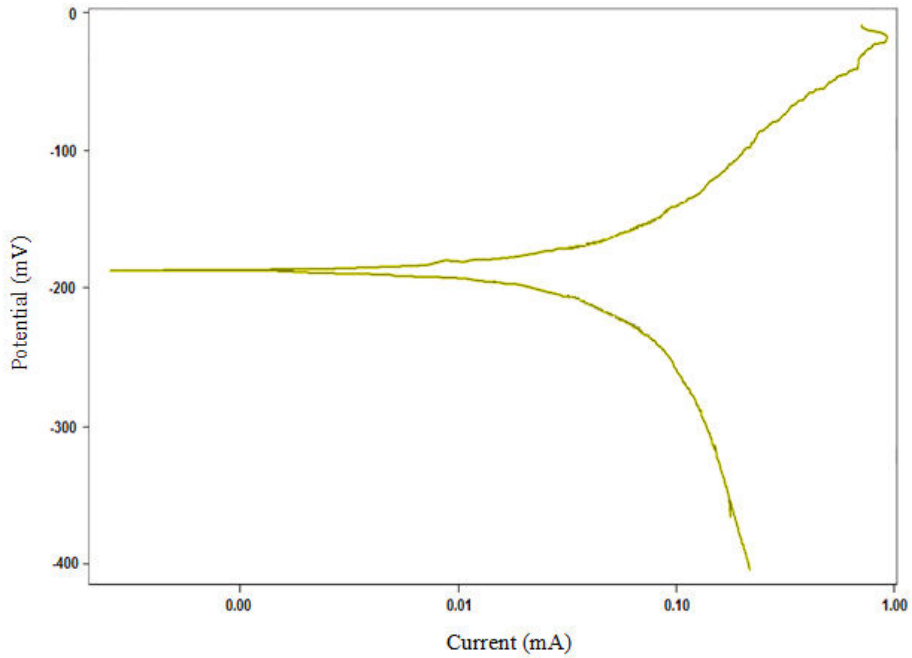

(a)

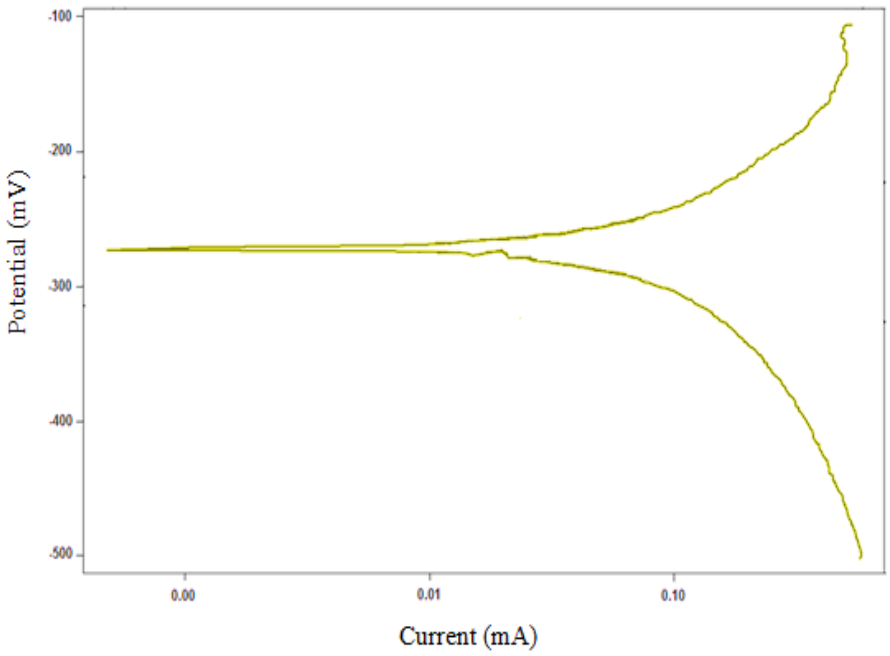

(b)

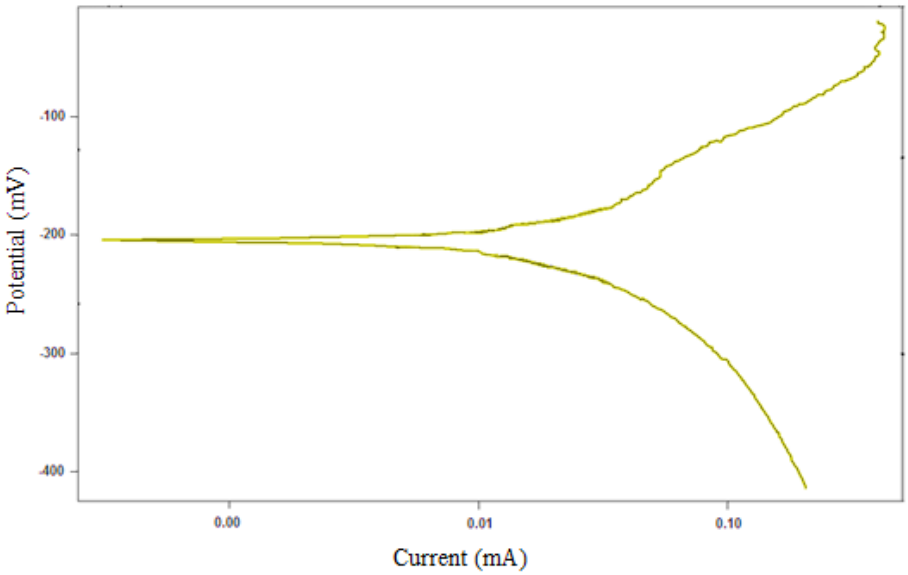

(c)

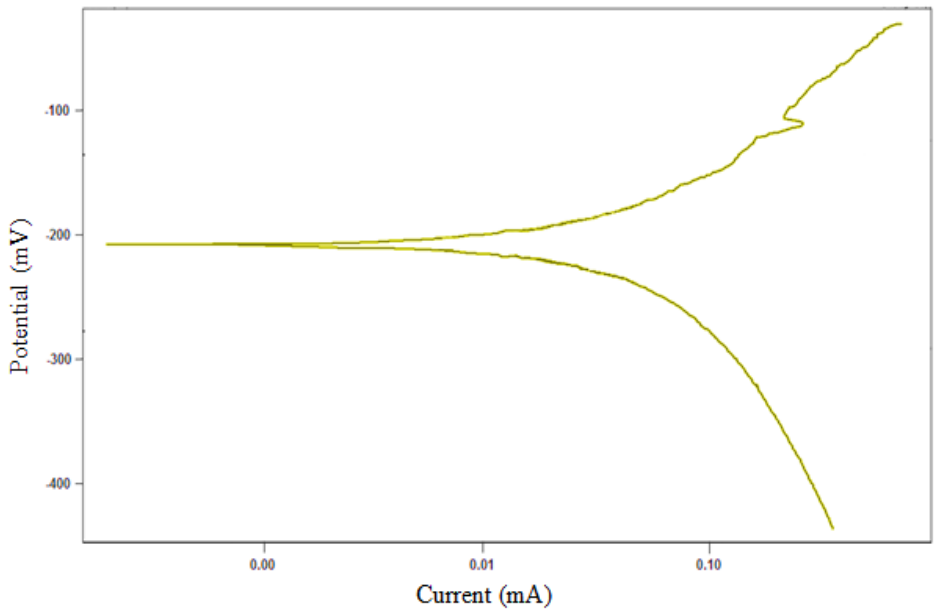

(d)

Figure-9. Potentiodynamic polarization for (a) base alloy and Ti-5Al-2.5Fe-xMo alloys (b) 1Mo, (c) 2Mo and (d) 3Mo in Hank's solution.

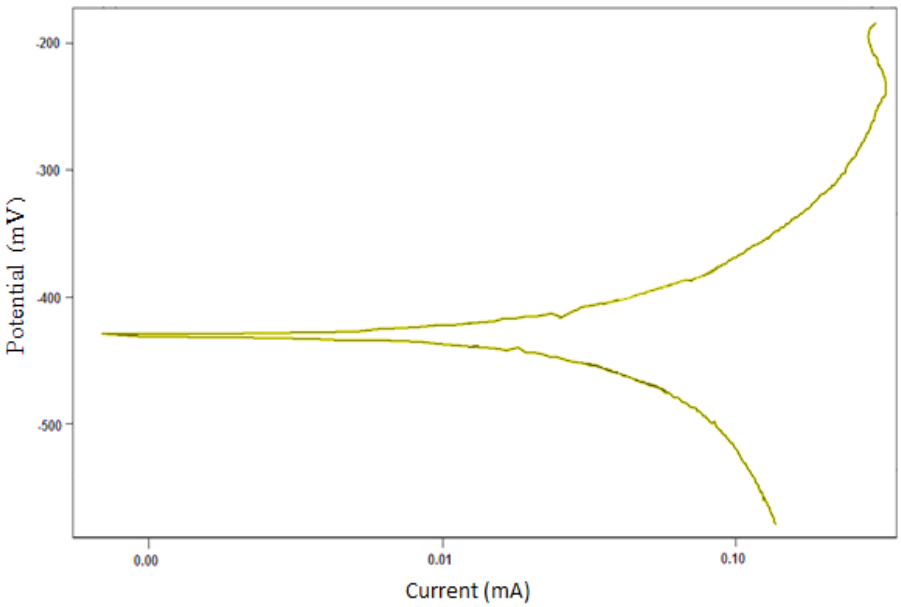

(a)

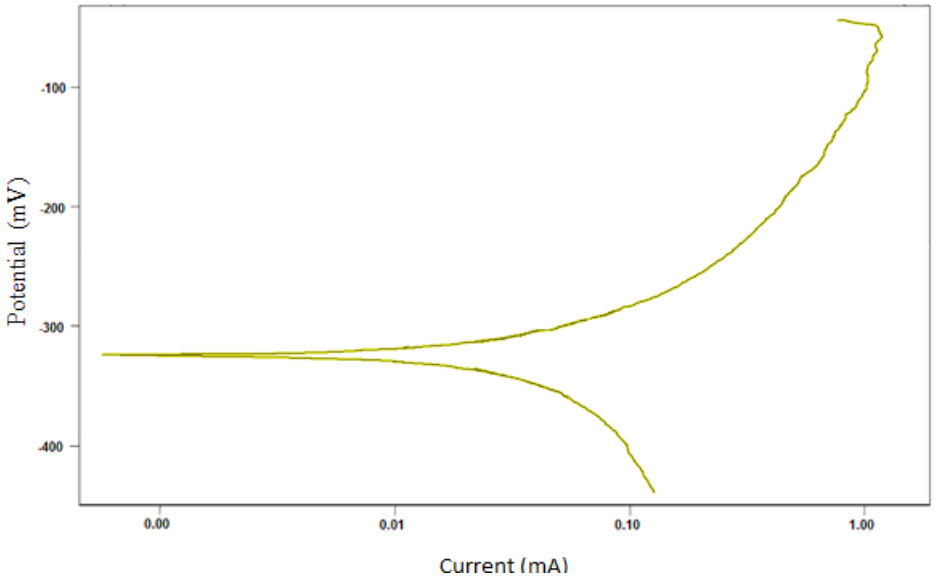

(b)

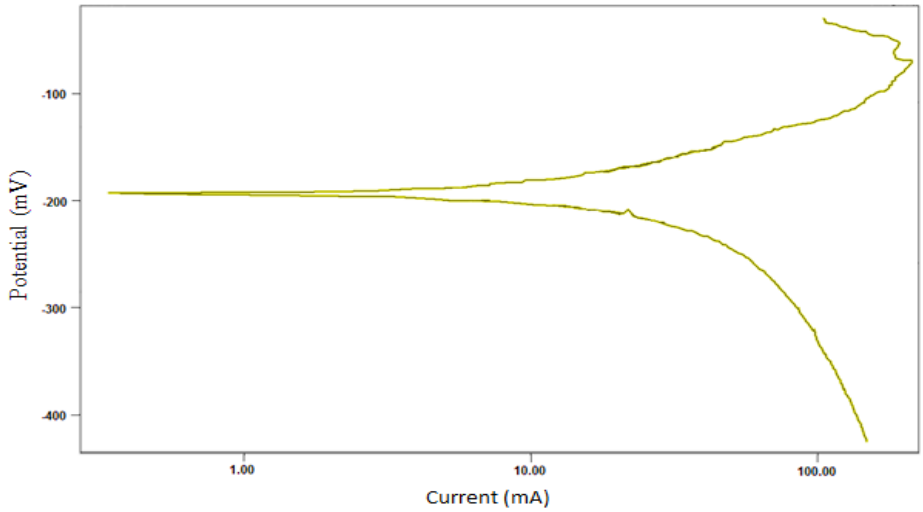

(c)

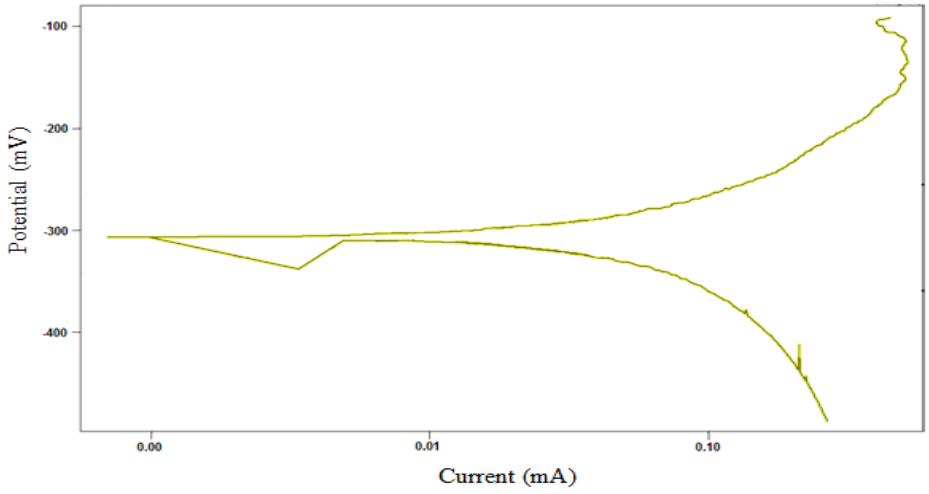

(d)

Figure-10. Potentiodynamic polarization for (a) base alloy and Ti-5Al-2.5Fe-xMo alloys (b) 1Mo, (c) 2Mo and (d) 3Mo in artificial saliva.

The microstructure for the corroded surface has been taken by using SEM in order to study the corrosion effect on the surface of the alloy.

Figure-11 observed that the color of the surface has changed because of the corrosion products, and from that color it can be estimated that the corrosion has occurred on the surface.

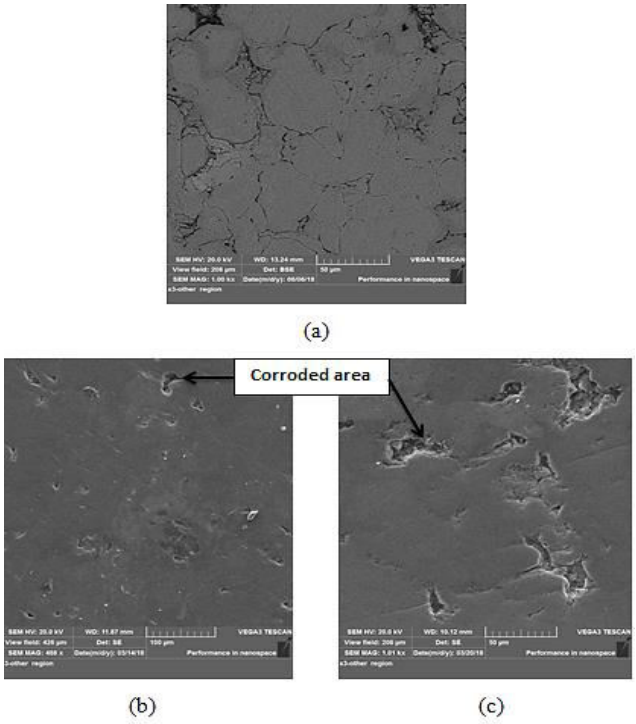

Figure-11. SEM for B alloy (a) uncorroded, (b) corroded in artificial saliva & (c) corroded in Hank's solution.

Figure-12 showed the microstructure for M3 alloy after the corrosion test in the two solutions (artificial saliva and Hank's solutions). The mentioned figures showed the changing in specimencolor due to corrosion products and absorbed on the pits which appeared on the surface especially in pores areas on the surface due to corrosion, because the pores represent a point defect which can be the direct cause for corrosion.

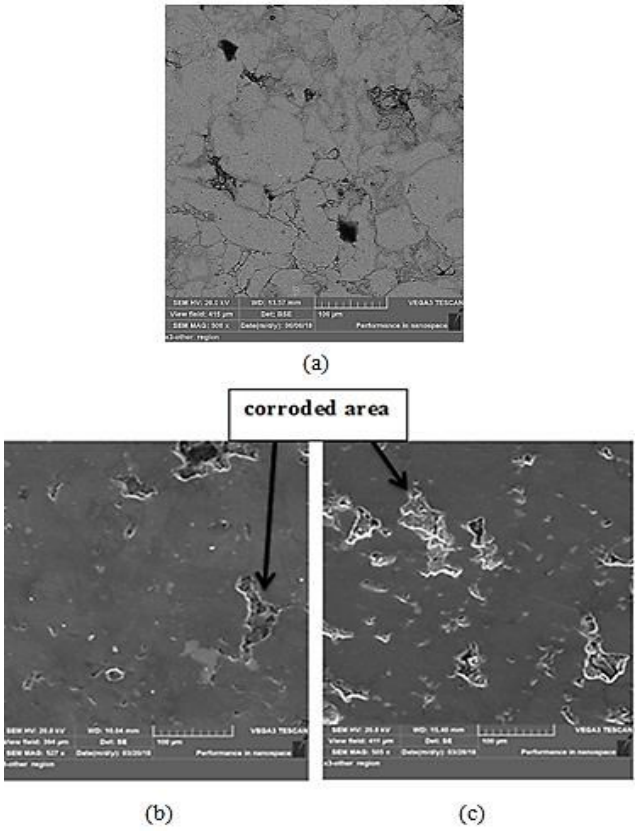

Figure-12. SEM for M3 alloy (a) uncorroded, (b) corroded in artificial saliva & (c) corroded in Hank's solution.

4. CONCLUSIONS

a) The electrochemical behavior of (Ti-5Al-2.5Fe-xMo) alloys were inspected in two body fluid solutions (artificial saliva and Hanks solutions) at 37°C±2 with low corrosion current density.

b) The Ti alloy such as (Ti-5Al-2.5Fe) with elements Mo exhibited enhance the passive layer that is protective and integral enough to a more area and that affect on corrosion result.

c) The corrosion rates obtained from the Tafel method provide a realistic comparison between (Ti-5Al-2.5Fe) and (Ti-5Al-2.5Fe-xMo).

d) Using optical microscopy and X-ray diffraction analysis, it was possible to verify the formation among others, of the phase α orβ.

ACKNOWLEDGEMENTS

The authors would like to acknowledge the support of this work by the department of Metallurgical Engineering/ Faculty of Materials engineering/ Babylon University.

REFERENCES

[1] Quan G.-Z., Wang X., Li Y.-L. and Zhang L. 2017. Analytical Descriptions of Dynamic Softening

Mechanisms for Ti-13Nb-13Zr Biomedical Alloyin Single Phase and Two Phase Regions. 62: 2029-2043.

[2] Liang C., Chang S.-H., Wang W.-D., Huang K.-T. and Lin S.-T. 2016. Change in Microstructure, Mechanical Strength and Corrosion Resistance of Ti-8Mo-xNi Alloys through Various Sintering Temperatures. 57(8): 1363-1369.

[3] Ferreiraa C.C., Riccia V.P., de Sousaa L.L. 2017. Improvement of Titanium Corrosion Resistance by Coating with Poly-Caprolactone and Poly-Caprolactone/Titanium Dioxide: Potential Application in Heart Valves, 20, pp. 126-133.

[4] Singh A., Singh B P, Wani M.R, Kumar D., Singh J K and Singh V. 2013. Effect of Anodization on Corrosion Behaviour and Biocompatibility of Cp-Titanium in Simulated Body Fluid. 36(5): 931-937.

[5] Siqueira R.P., Sandim H.R.Z, Hayama A.O.F., Henriques V.A.R. 2015. Dissolution of Intermetallic Powders during Sintering of the Blended Elemental Ti-5Al-2.5Fe Alloy. no. 03 February.

[6] Park J., Jeong G., Kang S., Lee S.J., Choi H. 2015. Fabrication of Fe-Cr-Mo powder metallurgy steel via a mechanical-alloying process. Metals and Materials International. 21(6): 1031-1037.

[7] Bolzoni L., Ruiz-Navas E.M., Neubauer E., Gordo E. 2012. Mechanical properties and microstructural evolution of vacuum hot-pressed titanium and Ti–6Al-7Nb alloy. Journal of the Mechanical Behavior of Biomedical Materials. 9, pp. 91-99.

[8] Bolzoni L., Ruiz-Navas E.M., Gordo E. 2015. Feasibility study of the production of biomedical Ti–6Al–4V alloy by powder metallurgy. Materials Science and Engineering. 49, pp. 400-407.

[9] Tahir A.M. 2014. Alloy element redistribution during sintering of powder metallurgy steels. 26, May, p. 1.

[10] Siqueira R. P., Sandim H. R. Z., Hayama A. O. F. and Henriques V. A. R. 2015. Dissolution of Intermetallic Powders during Sintering of the Blended Elemental Ti-5Al-2.5Fe Alloy, 3.

[11] Yamanoglu R., Efendi E. and Daoud I. 2017. Sintering Properties of Mechanically Alloyed Ti-5Al-2.5Fe. World Academy of Science, Engineering and Technology. International Journal of Chemical, Molecular, Nuclear, Materials and Metallurgical Engineering. 11(5): 360-364.

[12] Kim D.H Won J.W., Jeong D.W., Lee H.S., Yoon S.Y. and Hyun Y.T. 2017. Effect of Oxygen Content on the Phase Transformation of Ti-5Al-2.5 Fe Alloy during Continuous Cooling. Korean Journal of Metals and Materials. 55(9): 600-608.

[13] Yamanoglu R., Efendi E., Kolayli F., Uzuner H. and Daoud I. 2018. Production and mechanical properties of Ti–5Al–2.5 Fe–xCu alloys for biomedical applications. Biomedical Materials. 13(2): 025013.

[14] Dai N., Zhang L.C., Zhang J., Chen Q. and WuM. 2015. Corrosion Behaviour of Selective Laser MeltedTi-6Al-4V Alloy in NaCl Solution. 6027, Australia.

[15] Dawood N. M. 2014. Preparation and Characterization of Bio Nitinol with Addition of Copper. PhD. thesis, materials engineering department, university of technology/ Iraq.

[16] Jabber H. H. 2014. The Effect of Add mixed Ti on Corrosion Resistant of High Copper Dental Amalgam. Journal of Babylon University. 22(2): 413-421.

[17] Li Y., Yang C., Zhao H., Qu S., Li X. and Li Y. 2014. New Developments of Ti-Based Alloys for Biomedical Applications. 7: 1709-1800.

[18] Secchi V., Franchi S., Santi M., Vladescu A., Braic M., Skála T., Nováková J., Dettin M., Zamuner A., Iucci G. and Battocchio C. 2018. Biocompatible Materials Based on Self-Assembling Peptides on Ti25Nb10Zr Alloy: Molecular Structure and Organization Investigated by Synchrotron Radiation Induced Techniques. 8, 148; doi: 10.3390.

[19] Thirumalaikumarasamy D., Shanmugam K., Balasubramanian V. 2014. Comparison of the corrosion behaviour of AZ31B magnesium alloy under immersion test and potentiodynamic polarization test in NaCl solution. 28.